Author Manuscript

Globally, tree fecundity exceeds productivity gradients

—

Valentin Journé,[1] Robert Andrus,[2] Marie-Claire Aravena,[3] Davide Ascoli,[4] Roberta Berretti,[4] Daniel Berveiller,[5] Michal Bogdziewicz,[6] Thomas Boivin,[7] Raul Bonal,[8] Thomas Caignard,[9] Rafael Calama,[10] J. Julio Camarero,[11] Chia-Hao Chang-Yang,[12] Benoit Courbaud,[1] Francois Courbet,[7] Thomas Curt,[13] Adrian J. Das,[14] Evangelia Daskalakou,[15] Hendrik Davi,[7] Nicolas Delpierre ,[5] Sylvain Delzon,[9] Michael Dietze,[16] Sergio Donoso Calderon,[3] Laurent Dormont,[17] Josep Maria Espelta,[18] Timothy J. Fahey,[19] William Farfan-Rios,[20] Catherine A. Gehring,[21] Gregory S. Gilbert,[22] Georg Gratzer,[23] Cathryn H. Greenberg,[24] Qinfeng Guo,[25] Andrew Hacket-Pain,[26] Arndt Hampe ,[9] Qingmin Han,[27] Janneke Hille Ris Lambers,[28] Kazuhiko Hoshizaki,[29] Ines Ibanez,[30] Jill F. Johnstone,[31] Daisuke Kabeya,[27] Roland Kays,[32] Thomas Kitzberger,[33] Johannes M.H. Knops,[34] Richard K. Kobe,[35] Georges Kunstler,[1] Jonathan G.A. Lageard,[36] Jalene M. LaMontagne,[37] Theodor Leininger,[38] Jean-Marc Limousin,[39] James A. Lutz,[40] Diana Macias,[41] Eliot J.B. McIntire,[42] Christopher M. Moore,[43] Emily Moran,[44] Renzo Motta,[4] Jonathan A. Myers,[45] Thomas A. Nagel,[46] Kyotaro Noguchi,[47] Jean-Marc Ourcival ,[39] Robert Parmenter,[48] Ian S. Pearse,[49] Ignacio M. Perez-Ramos,[50] Lukasz Piechnik,[51] John Poulsen,[52] Renata Poulton-Kamakura,[52] Tong Qiu,[52] Miranda D. Redmond,[53] Chantal D. Reid,[52] Kyle C. Rodman,[54] Francisco Rodriguez-Sanchez,[55] Javier D. Sanguinetti ,[56] C. Lane Scher,[52] Harald Schmidt Van Marle,[3] Barbara Seget,[51] Shubhi Sharma,[52] Miles Silman,[57] Michael A. Steele,[58] Nathan L. Stephenson,[14] Jacob N. Straub,[59] Jennifer J. Swenson,[52] Margaret Swift,[52] Peter A. Thomas,[60] Maria Uriarte,[61] Giorgio Vacchiano,[62] Thomas T. Veblen,[2] Amy V. Whipple,[63] Thomas G. Whitham,[63] Boyd Wright,[64] S. Joseph Wright,[65] Kai Zhu,[22] Jess K. Zimmerman,[66] Roman Zlotin,[67] Magdalena Zywiec,[51] and James S. Clark,[1,52]

[1]Universite Grenoble Alpes, Institut National de Recherche pour Agriculture, Alimentation et Environnement (INRAE), Laboratoire EcoSystemes et Societes En Montagne (LESSEM), 38402 St. Martin-d'Heres, France.

[2]Department of Geography, University of Colorado Boulder, Boulder, CO 80309 USA.

[3]Universidad de Chile, Facultad de Ciencias Forestales y de la Conservacion de la Naturaleza (FCFCN), La Pintana, 8820808 Santiago, Chile.

[4]Department of Agriculture, Forest and Food Sciences, University of Torino, 10095 Grugliasco, TO, Italy.

[5]Universite Paris-Saclay, Centre national de la recherche scientifique, AgroParisTech, Ecologie Systematique et Evolution, 91405 Orsay, France.

[6]Department of Systematic Zoology, Faculty of Biology, Adam Mickiewicz University, Umultowska 89, 61-614 Poznan, Poland.

[7]Institut National de Recherche pour Agriculture, Alimentation et Environnement (INRAE), Ecologie des Forets Mediterranennes, 84000 Avignon, France.

[8]Department of Biodiversity, Ecology and Evolution, Complutense University of Madrid, 28040 Madrid, Spain.

[9]Universite Bordeaux, Institut National de Recherche pour Agriculture, Alimentation et Environnement (INRAE), Biodiversity, Genes, and Communities (BIOGECO), 33615 Pessac, France.

[10]Centro de Investigacion Forestal (INIA-CSIC), 28040 Madrid, Spain .

[11]Instituto Pirenaico de Ecologla, Consejo Superior de Investigaciones Cientificas (IPE-CSIC), 50059 Zaragoza, Spain.

[12]Department of Biological Sciences, National Sun Yat-sen University, Kaohsiung 80424, Taiwan.

[13]Aix Marseille universite, Institut National de Recherche pour Agriculture, Alimentation et Environnement (IN-RAE), 13182 Aix-en-Provence, France.

[14]USGS Western Ecological Research Center, Three Rivers, CA, 93271 USA.

[15]Institute of Mediterranean and Forest Ecosystems, Hellenic Agricultural Organization ḊEMETER, 11528 Athens, Greece.

[16]Earth and Environment, Boston University, Boston, MA, 02215 USA.

[17]Centre d'Ecologie Fonctionnelle et Evolutive (CEFE), Centre National de la Recherche Scientifique (CNRS), 34293 Montpellier, France..

[18]Centre de Recerca Ecologica i Aplicacions Forestals (CREAF), Bellaterra, Catalunya 08193, Spain.

[19]Natural Resources, Cornell University, Ithaca, NY, 14853 USA.

[20]Washington University in Saint Louis, Center for Conservation and Sustainable Development, Missouri Botanical Garden, St. Louis, MO 63110 USA.

[21]Department of Biological Sciences and Center for Adaptive Western Landscapes.

[22]Department of Environmental Studies, University of California, Santa Cruz, CA 95064 USA.

[23]Institute of Forest Ecology, Peter-Jordan-Strasse 82, 1190 Wien, Austria.

[24]Bent Creek Experimental Forest, USDA Forest Service, Asheville, NC 28801 USA.

[25]Eastern Forest Environmental Threat Assessment Center, USDA Forest Service, Southern Research Station, Research Triangle Park, NC 27709 USA.

[26]Department of Geography and Planning, School of Environmental Sciences, University of Liverpool, Liverpool, United Kingdom.

[27]Department of Plant Ecology Forestry and Forest Products Research Institute (FFPRI), Tsukuba, Ibaraki, 305-8687 Japan.

[28]Department of Environmental Systems Science, ETH Zurich, Switzerland 8092.

[29]Department of Biological Environment, Akita Prefectural University, Akita 010-0195, Japan.

[30]School for Environment and Sustainability, University of Michigan, Ann Arbor, MI 48109.

[31]Institute of Arctic Biology, University of Alaska, Fairbanks, AK 99700, USA.

[32]Department of Forestry and Environmental Resources, NC State University, Raleigh, NC USA.

[33]Department of Ecology, Instituto de Investigaciones en Biodiversidad y Medioambiente (Consejo Nacional de Investigaciones Cientificas y Tecnicas - Universidad Nacional del Comahue), Quintral 1250, 8400 Bariloche, Argentina.

[34]Health and Environmental Sciences Department, Xian Jiaotong-Liverpool University, Suzhou, China, 215123.

[35]Department of Plant Biology, Program in Ecology, Evolutionary Biology, and Behavior, Michigan State University, East Lansing, MI 48824.

[36]Department of Natural Sciences, Manchester Metropolitan University, Manchester M1 5GD, UK.

[37]Department of Biological Sciences, DePaul University, Chicago, IL 60614 USA.

[38]USDA, Forest Service, Southern Research Station, PO Box 227, Stoneville, MS 38776.

[39]CEFE, Univ Montpellier, CNRS, EPHE, IRD, 1919 route de Mende, 34293 Montpellier Cedex 5, France.

[40]Department of Wildland Resources, and the Ecology Center, Utah State University, Logan, UT 84322 USA.

[41]Department of Biology, University of New Mexico, Albuquerque, NM 87131 USA.

[42]Pacific Forestry Centre, Victoria, British Columbia, V8Z 1M5 Canada.

[43]Department of Biology, Colby College, Waterville, ME 04901 USA.

[44]School of Natural Sciences, UC Merced, Merced, CA 95343 USA.

[45]Department of Biology, Washington University in St. Louis, St. Louis, MO.

[46]Department of forestry and renewable forest resources, Biotechnical Faculty, University of Ljubljana, Ljubljana, Slovenia.

[47]Tohoku Research Center, Forestry and Forest Products Research Institute, Morioka, Iwate, 020-0123, Japan.

[48]Valles Caldera National Preserve, National Park Service, Jemez Springs, NM 87025 USA.

[49]Fort Collins Science Center, 2150 Centre Avenue, Bldg C, Fort Collins, CO 80526 USA.

[50]Inst. de Recursos Naturales y Agrobiologia de Sevilla, Consejo Superior de Investigaciones Cientificas (IRNAS-CSIC), Seville, Andalucia, Spain.

[51]W. Szafer Institute of Botany, Polish Academy of Sciences, Lubicz 46, 31-512 Krakow, Poland.

[52]Nicholas School of the Environment, Duke University, Durham, NC 27708 USA.

[53]Department of Forest and Rangeland Stewardship, Colorado State University, Fort Collins, CO, USA.

[54]Department of Forest and Wildlife Ecology, University of Wisconsin-Madison, Madison, WI 53706 USA.

[55]Department of Biologia Vegetal y Ecologia, Universidad de Sevilla, 41012 Sevilla, Spain.

[56]Bilogo Dpto. Conservacin y Manejo Parque Nacional Lanin Elordi y Perito Moreno 8370, San Marten de los Andes Neuqun Argentina.

[57]Department of Biology, Wake Forest University, 1834 Wake Forest Rd, Winston-Salem, NC 27106 USA.

[58]Department of Biology, Wilkes University, 84 West South Street, Wilkes-Barre, PA 18766 USA.

[59]Department of Environmental Science and Ecology, State University of New York-Brockport, Brockport, NY 14420 USA.

[60]School of Life Sciences, Keele University, Staffordshire ST5 5BG, UK.

[61]Department of Ecology, Evolution and Environmental Biology, Columbia University, 1113 Schermerhorn Ext., 1200 Amsterdam Ave., New York, NY 10027.

[62]Department of Agricultural and Environmental Sciences - Production, Territory, Agroenergy (DISAA), University of Milan, 20133 Milano, Italy.

[63]Department of Biological Sciences, Northern Arizona University, Flagstaff, AZ 86011 USA.

[64]Botany, School of Environmental and Rural Science, University of New England, Armidale, NSW, 2350, Australia.

[65]Smithsonian Tropical Research Institute, Apartado 0843n03092, Balboa, Republic of Panama.

[66]Department of Environmental Sciences, University of Puerto Rico, Rio Piedras, PR 00936 USA.

[67]Geography Department and Russian and East European Institute, Bloomington, IN 47405 USA

—-

keywords: climate | competition | forest regeneration | seed consumption | species interactions | tree fecundity

Short running title: Global trends in tree fecundity

Type of article: Letter #Total word count abstract: 132 #Total word count main text: ~ 3900 #Total word count figure legends: ~ 500 # 67 references # 0 Table and 6 Figures (color) # 1 Supporting information

Data availability statement

All data and code supporting our results are archived on the Zenodo Repository at the following link: https://doi.org/10.5281/zenodo.6381799

Author contributions

V.J. and J.S.C performed analyses and co-wrote the paper, J.S.C. designed the study, compiled the MASTIF network, and wrote the MASTIF model and software, M.B, B.C, G.K, and T.Q. co-wrote the paper, and all authors contributed data and revised the paper.

Abstract

Lack of tree fecundity data across climatic gradients precludes analysis of how seed supply contributes to global variation in forest regeneration and biotic interactions responsible for biodiversity. A global synthesis of raw seed-production data shows a 250-fold increase in seed abundance from cold-dry to warm-wet climates, driven primarily by a 100-fold increase in seed production for a given tree size. The modest (three-fold) increase in forest productivity across the same climate gradient cannot explain the magnitudes of these trends. The increase in seeds per tree can arise from adaptive evolution driven by intense species interactions or from the direct effects of a warm, moist climate on tree fecundity. Either way, the massive differences in seed supply ramify through food webs potentially explaining a disproportionate role for species interactions in the wet tropics.

Introduction

Understanding how tree fecundity contributes to global biodiversity and ecosystem function requires estimates of latitudinal trends in seed production. At the community scale, tree fecundity determines the density of competing offspring and the diets of consumers and seed dispersers that depend on seeds and seedlings (Terborgh, 1986; Corlett, 2013; Mokany *et al.*, 2014). Diversity, stem density, and growth and mortality rates all show important trends with latitude (Phillips & Gentry, 1994; Lewis *et al.*, 2004; Stephenson & Van Mantgem, 2005; Chu *et al.*, 2019; Locosselli *et al.*, 2020). Fecundity estimates are now available in North America (Clark *et al.*, 2021; Sharma *et al.*, 2021), but unlike growth and mortality rates (Stephenson & Van Mantgem, 2005; Brienen *et al.*, 2020), fecundity estimates have not been compiled from the tropics. At the global scale, a meta-analysis of 18 seed-trap studies in temperate and tropical forests did not find a relationship between seed-rain density (seeds per area) and latitude, but the same study suggested that seed-mass density might decline with latitude (Moles *et al.*, 2009). If the density of seed mass per-area is higher in the tropics than the temperate zone, does high seed mass density in the tropics come from the fact that tropical trees are simply larger and/or embedded in more productive communities, as assumed in Dynamic Global Vegetation Models (DGVMs) (Sitch *et al.*, 2003; Krinner *et al.*, 2005; Fisher *et al.*, 2018; Hanbury-Brown *et al.*, 2022)? Alternatively, does high seed mass density in the tropics result from greater seed production for a given tree size? Understanding global trends requires estimates of seed-production at both the individual-tree and the per-area scales. We present a new synthesis that allows us to quantify the fecundity gradient on a global scale and determine that the fecundity gradient is amplified in warm/moist climates beyond what can be explained by tree size or NPP.

The global meta-analysis that found a possible trend in seed mass multiplied the number of seeds counted in traps by the average seed size for all plant species that were observed at the same latitude (Moles *et al.*, 2009). Authors recognized the approximate nature of these estimates given the seven-order of magnitude range of seed sizes used to obtain the latitude means. In addition to uncertain seed size, counts from seed traps vary widely depending on precise placement of seed traps relative to locations of trees. Where reproduction is counted directly on trees, studies typically report on one to a few species from one to a few sites, and not seed production for all trees in measured plots, as would be needed to place fecundity on a per-area basis. Recent compilations of year-to-year mast production recognise additional challenges posed by divergent methods, some yielding a range of indices at the individual or stand scale on relativized or ordinal scales (LaMontagne *et al.*, 2020; Pearse *et al.*, 2020). Unlike previous meta-analyses, we analyze raw data referenced to an individual tree-year, i.e., the seed production

Figure 1: a) Individual seed productivity (ISP, seed mass per tree basal area) might not vary with latitudinal climate gradients, in which case community seed productivity (CSP, seed mass production per forest area) depends on variation in tree size. Alternatively, responses could depend on net primary productivity (NPP), increasing if allocation in warm climates shifts preferentially to fecundity or decreasing if allocation in warm climates shifts to growth and defenses. b) Proportionate differences in fecundity hypothesized for the three scenarios in (a) shown as differences from the climate gradient in NPP. The NPP-scaling scenario means that NPP and CSP follow the same proportionate trajectory (green line).

179 by each tree in each year, including all trees on inventory plots. By estimating seed production
180 at the tree-year scale (Clark *et al.*, 2019) we quantify both the trends in individual production
181 and in the seed production per area.
182   The indicators that we evaluate allow us determine both the gradient in seed productivity of
183 communities and how the gradient in seed productivity is influenced by individual tree responses.
184 Individual fecundity could vary due to climate through alternative allocation priorities (Fig. 1a).
185 Because reproductive effort depends on both seed sizes and numbers (Westoby *et al.*, 1992), and
186 reproductive effort varies with tree size (Qiu *et al.*, 2021), *individual standardized production*

187 (ISP) is d

188 (g m^{-2}yr^{-}
189 of mean s
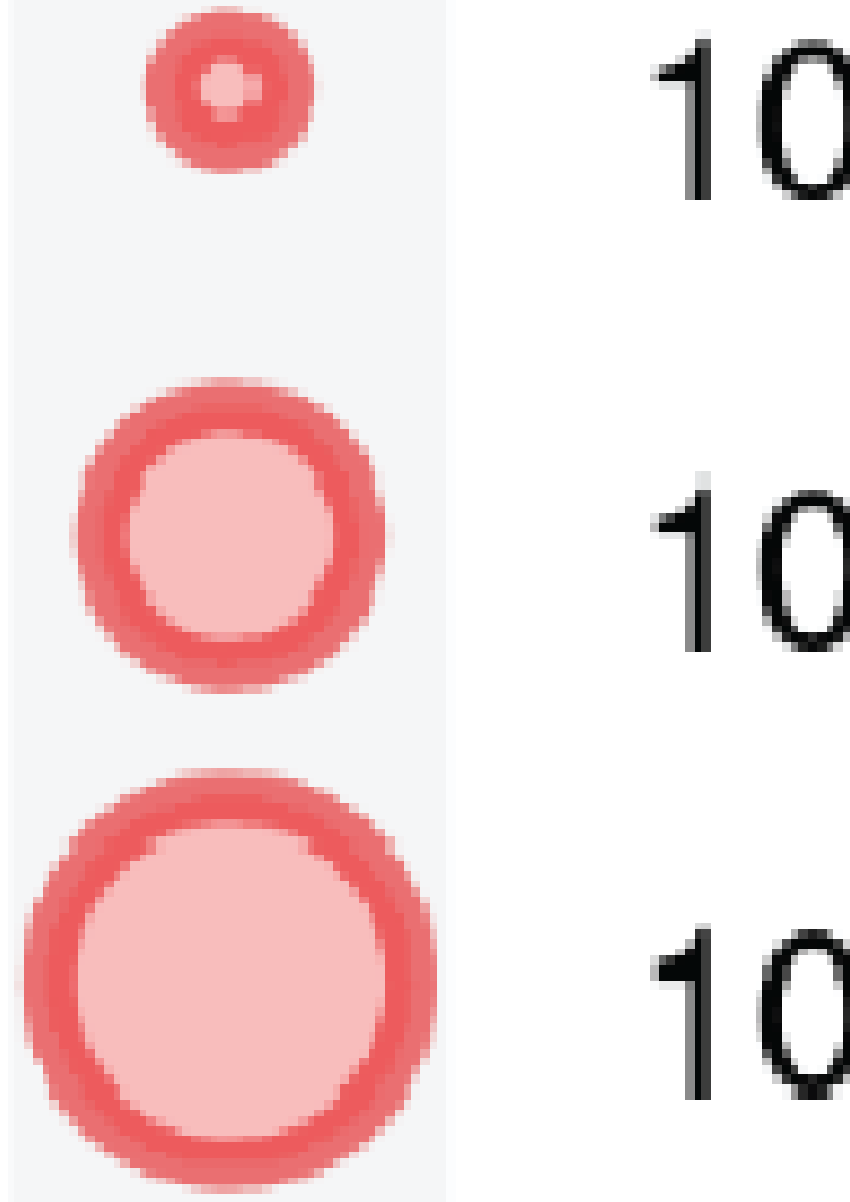190 neighbors
191 Uncertain
192 difference
193 assumed i
194 size still
195 and thus s
196 across the
197 response
198 climates (

Figure 2: MASTIF data summary, with symbol size proportional to observations. The distribution of data is detailed in Figure S1 and in Table S1.

199   While ISP$_{ij}$ can show how individual allocation changes with climate, *community seed*
200 *production*, CSP$_j$, quantifies seed production per area of forest, the starting point both for
201 stand regeneration and the interactions between seeds, seedlings, consumers, and dispersers.

[We hereafter omit subscripts to reduce clutter.] Like NPP, CSP is a community property, defined as the seed production summed over all trees on a plot and divided by plot area (g ha^{-1} yr^{-1}, Methods, eqn 5). CSP might scale as a fraction of NPP, as suggested by some empirical evidence (Vacchiano *et al.*, 2018) and assumed in DGVMs (Fisher *et al.*, 2018; Hanbury-Brown *et al.*, 2022). NPP scaling predicts high CSP in warm/moist climates where NPP is high (Del Grosso *et al.*, 2008) (Fig. 1b). It is also possible that intense competition selects for allocation to growth and defenses that enhance survival. If so, CSP is expected to show a flatter response to climate than the NPP response to climate ("↑growth/defense in Fig. 1).

Alternatively, fecundity responses could be amplified beyond what could be explained by the effects of climate on size or NPP ("↑fecundity" in Figure 1). There are at least two potential causes for fecundity amplification, including i) reproductive allocation can respond to favorable climates because reproduction is unconstrained by the structural and hydraulic constraints that limit growth responses (Koch *et al.*, 2004; King *et al.*, 2009), and ii) intense species interactions in the wet tropics amplify selection for reproduction to offset high losses to consumers and enhance the benefits of frugivory (Terborgh, 1986; Harms *et al.*, 2000; Hille Ris Lambers *et al.*, 2002; Schemske *et al.*, 2009; Levi *et al.*, 2019; Hargreaves *et al.*, 2019).

Large data sets are needed to estimate climate effects due to wide variation in seed production. For a given tree, large crop years often exceed intervening years by orders of magnitude (Mendoza *et al.*, 2018; Vacchiano *et al.*, 2018; LaMontagne *et al.*, 2020; Koenig, 2021). Variation between trees also varies by orders of magnitude (Clark *et al.*, 2004; Minor & Kobe, 2019). Seed production further responds to spatio-temporal variation in habitat and climate (Caignard *et al.*, 2017; Bogdziewicz *et al.*, 2020a), including local competition (Clark *et al.*, 2014, 2019). The many sources of variation means that biogeographic trends of interest can only be identified from broad coverage and large sample sizes, while accounting for individual tree condition, local habitat, and climate (Qiu *et al.*, 2021).

This synthesis extends the Masting Inference and Forecasting (MASTIF) network (Clark *et al.*, 2021; Sharma *et al.*, 2021) to quantify the climate controls on seed production globally and the extent to which seed-production trends go beyond what can be explained by effects of tree size and productivity. Data include 12M observations from 147K mature trees and 251 inventory plots (Fig. 2). We summarize climate trends with mean annual temperature and moisture surplus. Model fitting allows for the effects of individual condition and local habitat variation by including tree diameter, shade class, and soil cation exchange capacity (CEC), a widely used indicator of soil fertility (Hazelton & Murphy, 2007; Hengl *et al.*, 2017), all of which affect seed production (Materials and Methods).

Material and Methods

Fecundity Data

This study uses crop-count (CC, on trees) and seed-trap (ST) data (fig. 3) from the Masting Inference and Forecas project. Most observations (99%) come from longitudinal studies, where all trees on a plot (ST) or individual trees (CC) are observed repeatedly. Other CC observations (1%) are obtained opportunistically through the iNaturalist project MASTIF (Clark *et al.*, 2019). All observations provide estimates of ISP, including those on isolated trees. CSP requires seed production from a known area and comes from inventory plots (Table S1). Data include 12,053,732 tree-year observations from 748 species and 146,744 mature individuals.

As in all observational studies, geographic coverage is not uniform. The majority of sites are temperate (98%), while most observations (tree-years, 80%), trees (58%), and species (74%)

Figure 3: The MASTIF model simplified from Clark *et al.* (2019) to emphasize variables and parameters discussed in the text. A biophysical model for change in fecundity $\psi_{i,t}$ of tree i in year t (a tree-year) is driven by individual tree condition and climate and habitat variables in design vector $\mathbf{x}_{i,t}$ with corresponding coefficients $\boldsymbol{\beta}$. Maturation status incorporates tree diameter $d_{i,t}$. The hierarchical state-space model includes process error variance σ^2 and observation error in two data types. A crop count $c_{i,t}$ has a beta-binomial distribution that includes observation error through the estimated crop fraction. A set of seed traps provides a vector of counts $\mathbf{y}_t = y_{1,t}, \ldots, y_{n,t}$ that together provide information on tree i through a dispersal kernel. There is conditional independence in fecundity values between trees and within trees over time, taken up by stochastic treatment of $\psi_{i,t}$. There is an additional subscript for location j that is suppressed here to reduce clutter. The full model includes additional elements (see Model Inference with MASTIF).

are tropical. Sample sizes are included in Table S1. Sample locations are shown in Fig 2 and detailed in the Supplement (Figure S1 and Table S1). To assure that results are not dominated by any one site, we show that the same trends dominate when the largest tropical site, Barro Colorado Island (BCI), is removed from the analysis (Figure S4).

For both CC and ST data types, an observation references a tree-year (a fecundity estimate for one tree in one year). A crop-count (CC) observation includes the number of fruiting structures counted (e.g., individual seeds, cones, fruits) and an estimate of the fraction of the total crop represented by the count (see Model Inference with MASTIF). Where structures bear more than one seed, numbers are scaled by seeds per structure. For example, *Fagus* capsules bear two seeds per capsule, and *Pinus* cones bear from 10 to 200 seeds per cone, depending on species. Seed mass and number of seeds per fruiting structure were taken as an average for the species, obtained from collections in our labs, supplemented with the TRY Plant Trait Database (Kattge *et al.*, 2020). A seed-trap (ST) observation includes counts and locations for seed traps on an inventory plot where each tree is measured and mapped. The uncertainty in a tree-year estimate depends on the crop-fraction estimate for CC observations and on the redistribution

kernel for ST observations. A beta-binomial distribution for CC data combines uncertainty in the count and in the crop-fraction estimate. For ST observations, the redistribution model ("dispersal kernel") quantifies transport to seed traps, a categorical (multinomial) distribution allows for uncertain seed identification, and a Poisson likelihood allows for variable counts. These data models link to a common process model for individual fecundity (Figure 3). Stochastic treatment of fecundity absorbs dependence between observation types, between trees, and within trees over time. The full model is detailed in Clark *et al.* (2019) and summarized in the section Model Inference with MASTIF.

Environmental and Individual Covariates

Predictors for a given tree-year include diameter, crown class, climate, soil and terrain covariates (Table S2). Linear and quadratic terms for diameter allow for changes of fecundity with tree size (Qiu *et al.*, 2021). The crown class assigned to each tree ranges from 1 (full sun) to 5 (full shade), following the protocol used in the National Ecological Observation Network (NEON) and the USDA Forest Inventory and Analysis (FIA) program.

Climate variables include norms and annual anomalies for temperature (°C) from the previous year, and moisture surplus (summed monthly precipitation minus evapotranspiration, mm) from the previous and current years. To allow for changes in moisture access with tree size we included the interaction between moisture surplus and tree diameter. Climate variables were derived from CHELSA (Karger *et al.*, 2017), TerraClimate (Abatzoglou *et al.*, 2018), and local climate monitoring data where available. TerraClimate provides monthly but spatially coarse resolution (Abatzoglou *et al.*, 2018) through 2020. CHELSA provides high spatial resolution (1 km) but CHELSA is not available after 2016. We used regression to project CHELSA climate forward based on Terraclimate, followed by calibration to local weather data where available. Details are available in (Clark *et al.*, 2021).

Cation exchange capacity (CEC), an indicator of soil fertility (Hazelton & Murphy, 2007), was obtained from soilGrid250 (Hengl *et al.*, 2017) and used as the weighted mean from three soil depths: 0-5, 5-15 and 15-30 cm, where weights are the reported uncertainty values. Slope and aspect were obtained from the global digital elevation model from the NASA shuttle radar topography mission (Farr *et al.*, 2007) and, for latitudes above 61°, from the USGS National Elevation Dataset (Gesch *et al.*, 2002). Both products have 30-m resolution. The covariates for slope and aspect (u_1, u_2, u_3) constitute a length-3 vector,

$$\mathbf{u}_j = \begin{cases} u_{j,1} = \sin(s_j) \\ u_{j,2} = \sin(s_j)\sin(a_j) \\ u_{j,3} = \sin(s_j)\cos(a_j) \end{cases} \quad (2)$$

for slope s_j, where aspect a_j is taken in radians. These three terms are included as elements of the design vector $\mathbf{x}_{ij,t}$ (Clark, 1990b).

Model Inference with MASTIF

The MASTIF model is a (hierarchical) state-space, auto-regressive model that accommodates dependence between trees and within trees over years through a joint analysis detailed in Clark *et al.* (2019). For each tree i at location j and year t there is a mean fecundity estimate $\hat{f}_{ij,t} = \hat{\rho}_{ij,t}\hat{\psi}_{i,t}$ that is the product of conditional fecundity $\hat{\psi}$ and maturation probability $\hat{\rho}_{ij,t}$, which is the probability that an individual is in the mature state, $z_{ij,t} = 1$. The model for conditional fecundity is given by $\log\psi_{ij,t} = \mathbf{x}'_{ij,t}\boldsymbol{\beta}^{(x)} + \beta_i^{(w)} + \gamma_{g[i],t} + \epsilon_{i,t}$, where $\mathbf{x}_{ij,t}$ is the

design vector holding climate, soils, local crowding, and individual attributes (Table S2), $\boldsymbol{\beta}^{(x)}$ are fixed-effects coefficients, $\beta_i^{(w)}$ is the random effect for tree i, $\gamma_{g[i]j,t}$ are year effects that are random across groups g and fixed for year t, and $\epsilon_{ij,t}$ is Gaussian error. To approximate the scale of potential synchronicity of masting species, the group membership $g[i]$ for tree i is assigned by species-ecoregion (Clark *et al.*, 2019), using the WWF ecoregion classification (Olson *et al.*, 2001). The principle elements of the model are summarized as a directed acyclic graph (DAG) in fig. 3.

Conditional log fecundity ψ is censored at zero to allow for the immature state and for failed seed crops in mature individuals,

$$f_{ij,t}|(z_{ij,t}=1) = \begin{cases} 0 & \psi_{ij,t} \le 1 \\ \psi_{ij,t} & \psi_{ij,t} > 1 \end{cases} \tag{3}$$

This censoring means that seed production requires the potential to produce at least one seed; the Tobit model uses this censoring to allow for discrete zero observations for otherwise continuous response variables (Tobin, 1985). For ISP, fecundity is multiplied by mass per seed and standardized for tree basal area (eq. (1)). For CSP, seed mass is summed over trees on an inventory plot and divided by plot area. The uncertainty for both quantities is given in the section Uncertainty in ISP and CSP

The posterior distribution includes parameters and latent variables for maturation state and tree-year seed production. Posterior simulation uses direct sampling and Metropolis and Hamiltonian Markov Chain (HMC) updates within Gibbs. Model structure and methodology was implemented with R (version 4.0, R Core Team 2020) and the R package Mast Inference and Forecasting (MASTIF), detailed in Clark *et al.* (2019).

Uncertainty in ISP and CSP

Mean productivity estimates for an individual, ISP, incorporate year-to-year uncertainty for that tree. Mean productivity estimates for the community, CSP, incorporate tree-to-tree uncertainty for the inventory plot. We included only trees > 7 cm in diameter, i.e., at least as large as the smallest measured size in inventory data. Individual fecundity for species s at location j is evaluated as

$$\hat{f}_{ijs} = \frac{\sum_t w_{ijs,t}\hat{f}_{ijs,t}}{\sum_t w_{ijs,t}} \tag{4}$$

where the weight $w_{ijs,t}$ is the inverse of the predictive coefficient of variation for the estimate, $w_{ijs,t} = CV_{ijs,t}^{-1}$. Th CV is used rather than the predictive standard deviation, because the mean tends to scale with the variance such that a standard-deviation weight would have the undesirable property of down-weighting the important large values while up-weighting the less important low values. ISP combines fecundity from eq. (4) with seed mass and tree basal area in eq. (1).

Community seed production is evaluated from the individual means

$$CSP_j = \frac{n_j}{A_j} \frac{\sum_{is} w_{ijs}\hat{f}_{ijs}}{\sum_{is} w_{ijs}} \tag{5}$$

where A_j is plot area, n_j is the number of trees, and w_{ijs} is the inverse of the coefficient of variation given by the root mean predictive variance divided by the predictive mean for tree ijs. Because CSP requires plot area, only trees on inventory plots are included in the CSP analysis. Variation in ISP and CSP values were compared across temperature and moisture surplus using regression.

Net Primary Production

We extracted Net Primary Production (NPP) from the Moderate Resolution Imaging Spectrora-diometer (MODIS) product MOD17 at 500 m resolution (MOD17A3HGFv006, Running *et al.* 2004). We merged yearly CSP estimates with NPP from matching site years, which are available from 2000 to 2020. Because seed production data span the interval 1959 to 2020, we used the location-specific mean NPP values for the limited number of earlier years. Because MODIS NPP is influenced by cloud cover, we compared MODIS NPP values with NPP values from DGVMs in the S3 experiment of the TRENDY project (Sitch *et al.*, 2015). For each MASTIF site we averaged NPP from 11 models (CABLE-POP, CLASSIC, CLM5.0, ISAM, JSBACH, JULES, LPJ-GUESS, LPX, OCN, ORCHIDEE, ORCHIDEE-CNP) and fitted regressions to the same climate variables used for ISP and CSP (temperature, moisture surplus). The two NPP products show similar main effects, but differ in the temperature × moisture interaction, which is positive for MODIS and negative for the aggregated DGVM. Despite this difference in the interaction term, main effects dominate the response surfaces that show the same trends for both NPP sources (Figure S5). Thus, we included only MODIS results in Figure S6.

Results

Community seed production (CSP) increases 250-fold to a global maximum in the warm, moist tropics, primarily driven by a 100-fold increase in seed production for a given tree size (ISP). ISP and CSP trends with climate align with the geographic trend in NPP (panels in Fig. 4), but ISP and CSP far exceed the NPP response. The flat ISP (seed production per tree basal area) response expected if fecundity scales with tree basal area (Fig. 1) contrasts with the observed 100-fold ISP increase along this gradient (Fig. 5), verifying the amplification hypothesized in Figure 1b. The NPP-scaling assumed in current models (Fig. 1b) is likewise dwarfed by the CSP rise in seed supply to consumers (Fig. 4b).

Despite large trends in ISP and CSP with temperature and moisture (Fig. 5), the latitudinal contribution to fecundity variation is still lower than contributions of between-tree and the within-tree (over time) variation (Figure S2). Average seed production for 95% of all trees of a given size varies over five orders of magnitude, with ISP ranging from 0.000025 to 50 g per cm^2 of basal area (Figure S7a). Individual variation is matched by that for community seed production, with 95% of CSP values ranging from 50 g to 2500 kg ha^{-1} (Figure S7b). Tree-to-tree variation combines for an increase in ISP to highest values in warm, moist climates (Fig. 4a, b) that is driven more by temperature than by moisture (Table S3); the temperature response is amplified by moisture where temperatures are high (Figure S2c). The fact that the massive geographic trend in Fig. 5 can be masked by tree-to-tree and year-to-year variation (these sources are partitioned in Clark *et al.* 2004) emphasizes the importance of large data sets that span broad coverage in individual condition, habitat, and climate (Qiu *et al.*, 2021).

Forest productivity does not explain the global fecundity gradient evident at the individual and community levels. The parallel 100- and 250-fold increases for ISP and CSP (Fig. 5b) to maxima in warm, moist climates (Fig. 4) spans only a three-fold range for NPP. The trends in both ISP and CSP mean that not only do individual trees produce more seed for a given size in the wet tropics, but also that seed abundance is amplified at the community level (Figure 4a, b). [Community-level CSP need not necessarily track ISP responses due to heterogeneous size-species structures associated with local site conditions, past disturbance, and competition].

Discussion

The 250-fold latitudinal trend in tree seed production exceeds expectations from previous studies. The possibility that seed production might be highest at low latitudes and that seed production might not be explained by productivity was suggested from mean counts in 18 forest seed-trap studies (Moles *et al.*, 2009). New estimates reported here reflect an extension to large sample sizes, direct inference on seed production by each tree (rather than counts within traps), and use of seed mass for the species (rather than a mean value across all species at the same latitude). With synthetic modeling of 12M observations on 753 species we extend the previous discovery of a fecundity hotspot in the warm, moist southeastern North America (Clark *et al.*, 2021) to a global phenomenon.

Biogeographic trends reported here complement studies that focus on interannual variation, or "masting". Temporal variation in climate (Clark *et al.*, 2014; Caignard *et al.*, 2017; Bogdziewicz *et al.*, 2020a) are of great interest for understanding allocation shifts within individuals over time (Koenig, 2021), but these interactions fundamentally differ from geographic variation in populations subjected to divergent selection histories (Clark *et al.*, 2014). Results here provide a geographic context for variation within species and communities and the variables that control variation.

Improving forest regeneration in DGVMs might shift from the current focus on sharpening estimates of reproduction as a fraction of NPP (Fisher *et al.*, 2018; Hanbury-Brown *et al.*, 2022) to a recognition of how fecundity responses diverge from NPP. Results from figure 5 show that the DGVM assumption of fecundity as a simple fraction of NPP misses the key controls at stand and regional scales. Clearly, reproduction is not a residual sink to be filled after growth and other demands are satisfied. Previous understanding shows the assumption of reproduction as a constant fraction of NPP to be unrealistic at the individual scale (fecundity is far more volatile than annual resource capture or growth) (Clark *et al.*, 2004; Sala *et al.*, 2012; Clark *et al.*, 2014; Berdanier & Clark, 2016). The climate trends in Figure 5 show that NPP scaling also does not work as a community-level summary. Fecundity responses to local habitat and regional climate reported here can enter models directly.

Amplified fecundity in warm, moist climates, beyond what could be explained by trends in NPP (Fig. 5), may represent a direct climate response or the legacy of adaptive evolution to intense species interactions. By quantifying both individual and community seed productivity (ISP, CSP), we show that the community response is driven primarily by the fact that trees of a given size produce, on average, 100 times the seed mass in the wet tropics. This latitudinal trend in ISP is then amplified to a 250-fold trend in CSP (seed production per area) by the greater abundances of large trees in the wet tropics. Amplification beyond the trend in NPP may result from flexibility in seed production to respond to a longer growing season (Yeoh *et al.*, 2017; Mendoza *et al.*, 2018) well in excess of tree growth, which is limited by mechanical and hydraulic constraints on tree size (Koch *et al.*, 2004; King *et al.*, 2009). At the community scale, NPP is further constrained by the compensatory losses in stand biomass as mortality increases to offset increases in growth (Assmann, 1970; Clark, 1990a). Thus, while NPP increases with warm, wet conditions, the lack of structural constraints on producing more seeds might allow for a disproportionate fecundity response in Figure 1. Alternatively, amplification could also be driven by intense species interactions that select for reproduction to offset high losses to consumers and enhance the benefits of frugivory (Terborgh, 1986; Harms *et al.*, 2000; Hille Ris Lambers *et al.*, 2002; Schemske *et al.*, 2009; Levi *et al.*, 2019; Hargreaves *et al.*, 2019).

Whether amplification occurs as a direct response to climate or as an adaptive response to intense biotic interactions, the density- and frequency-dependent processes involving competition,
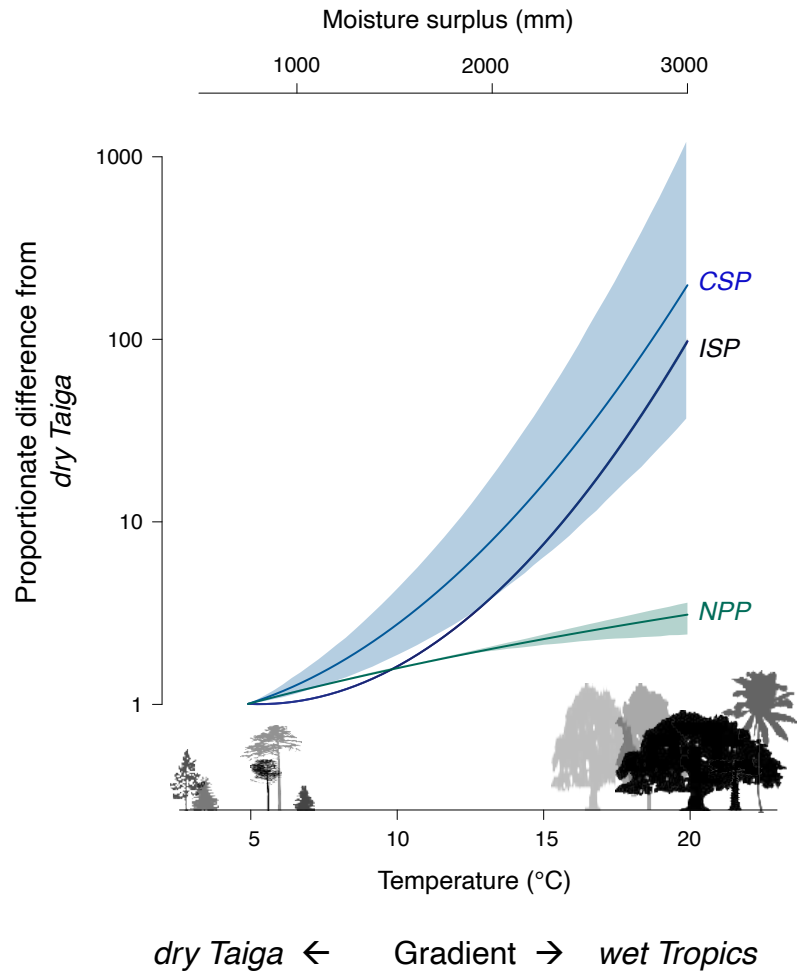
consumers, and seed dispersers have community-wide implications. The two order-of-magnitude climatic and latitudinal trend in seed mass per forest-floor area (CSP) has direct implications for density-dependent interactions, which include competition within tree species and frequency-dependent consumers. Elevated seed supply and the offsetting mortality losses affect selective pressure for competitive phenotypes. The bottom-up enrichment of food webs that cascades to higher trophic levels (Ostfeld & Keesing, 2000; Rosenblatt & Schmitz, 2016; Levi *et al.*, 2019) can increase consumer and disperser densities that, in turn, impose frequency-dependence selection on seed and seedling survival (Janzen, 1970). The magnitude of amplification suggests that seed supply intensifies species interactions in the wet tropics.

Frequency-dependent consumer pressures depend on diversity of the seed resource, which is poorly predicted by the standard inventory of trees. Using Shannon entropy $[-\sum_s p_s \log p_s$, where p_s is the fraction of species s in basal area (trees) and CSP (seed mass)], species diversity of both seed productivity and tree basal area is highest in the warm tropics. However, tree diversity exceeds the diversity of the seed resource in warm climates (Fig. 6). The lower species diversity for seeds than for trees in warm climates results from the fact that species having modest differences in tree basal area vary widely in fecundity; tendency for a subset of species to dominate seed production reduces seed diversity below that for trees. Conversely, in the cool climates where seeds tend to be small (small, blue symbols in Fig. 6), the low diversity that would be estimated on the basis of trees can mask an unexpectedly high seed diversity. Although many studies do not record fecundity for species having the smallest seeds (e.g., Salicaceae), these are also the seeds that are least apparent to many consumers. Omission of these smallest seeds from this study means that values of seed production are under-estimates, but still relevant for many consumers. The net effect of overestimating seed diversity in warm climates is important for frequency-dependent processes (Green *et al.*, 2014), such as host-specific seed predation.

Whether the 100-fold biogeographic gradient is driven by biophysical constraints on allocation or adaptive evolution to differing consumer pressures, these results add a new dimension to the understanding of trophic processes that may control latitudinal diversity gradients. If host-specific consumers regulate diversity through density- and frequency-dependent attack, then the strongest impacts are occurring where seed supply can support the highest numbers of consumers. Through shared consumers and frugivores, fecundity of many species can contribute to the selection pressures on competitors and consumers (Whitham *et al.*, 2020; Bogdziewicz *et al.*, 2020b). The dramatic biogeographic trend in seed supply sets up the potential for an evolutionary arms race (Dawkins & Krebs, 1979; Gruntman *et al.*, 2017) as selective pressures balance the benefits of producing more seed against the full costs of increased fecundity (Obeso, 2002; Pincheira-Donoso & Hunt, 2015; Fridley, 2017), including diverting resources from growth and defense (Berdanier & Clark, 2016; Lauder *et al.*, 2019). A positive feedback on selection pressure in diverse tropical forests could ensue where species from every major angiosperm clade enrich functional space and niche overlap. Regardless of whether this arms race has occurred, the trends in stand-level seed rain have profound implications for food web dynamics.

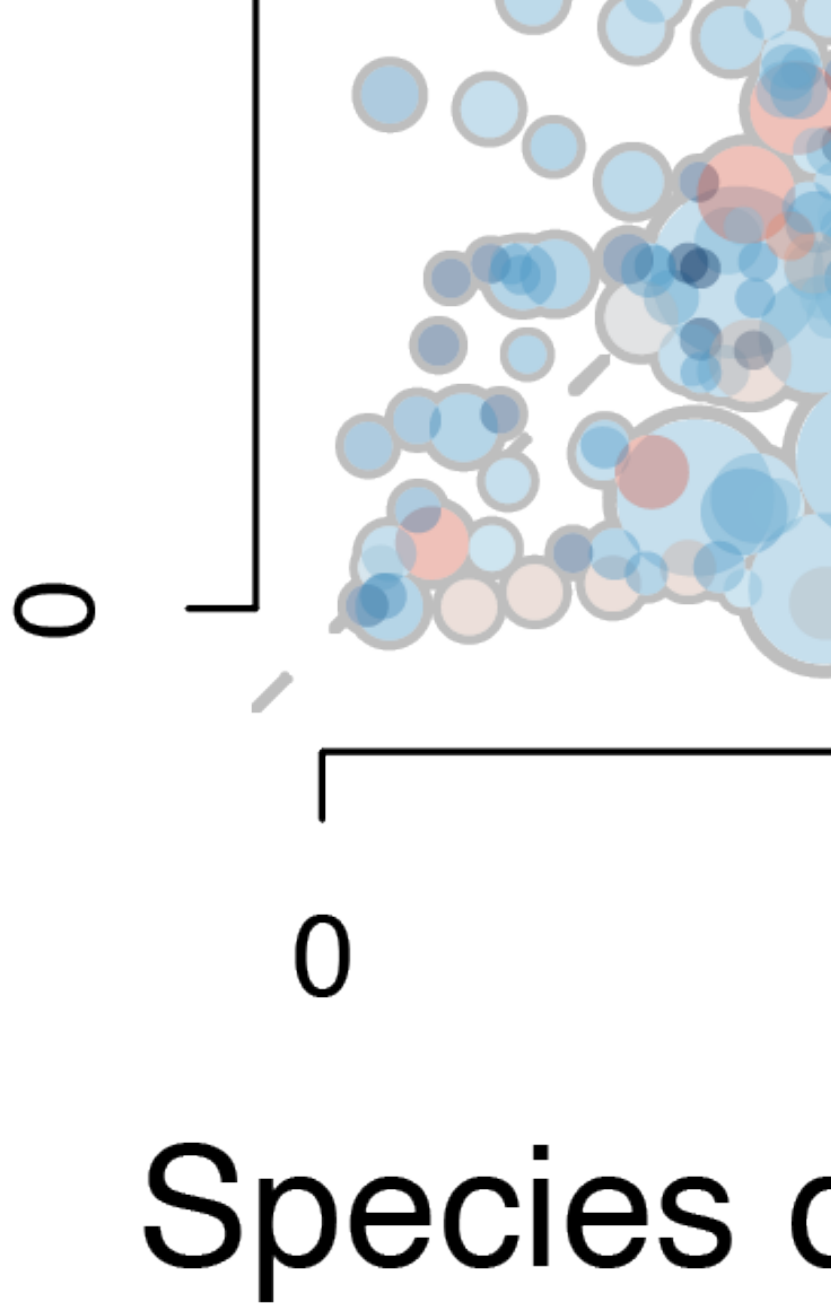Our results show that climate change impact on tree fecundity will not scale simply with change in productivity. Climate change induced changes in seed production will come with feedbacks through shared consumers and dispersers (Bogdziewicz *et al.*, 2020b). The temperature-tropical gradient in seed production reported here could motivate research on climate effect on seed production, their consumers and dispersers (Hargreaves *et al.*, 2019).

Figure 4: a) Climate responses for (a) ISP (seed production per tree basal area, $\log 10$ g m^{-2} y^{-1}) (b) CSP (seed mass per ha forest floor, $\log 10$ g ha^{-1} y^{-1}), and (c) NPP (kg C m^{-2} y^{-1}). Dashed lines indicate the transect from dry taiga to wet tropics in Fig. 5b. The scales for contours are linear for (c) and $\log_{10}$ for (a) and (b). Convex hulls are defined by observations (red), including individual trees (a, c) and inventory plots (b). Surface predictive standard error are reported in Figure S3. Coefficients are reported in Table S3.

Figure 5: a) Two order of magnitude increases from cold/dry to warm/moist for individual (ISP) and community (CSP) seed production relative to NPP. Curves are sections through surfaces (dashed lines) in Fig. 4, with scales for moisture surplus (above) and temperature (below). Curves are in proportion to values in cold, dry conditions. Confidence intervals (95%) are not visible for ISP and NPP due to the large number of trees. Confidence intervals are wider for CSP due to limited inventory plots at high temperatures (Fig. 2).

Figure 6: Species diversity in seeds (vertical axis) is lower than expected from species diversity in trees (horizontal axis). In both cases, diversity is evaluated from the Shannon index, $-\sum_s p_s \log p_s$, where p_s is the fraction of species s in basal area (trees) and CSP (seed mass). Each point represents an inventory plot. Except at low tree diversity, points lie almost entirely below the 1:1 line (dashed). The legend at top left shows mean annual temperature (symbol color) and mass of the average seed (symbol size).

References

Abatzoglou, J.T., Dobrowski, S.Z., Parks, S.A. & Hegewisch, K.C. (2018). Terraclimate, a high-resolution global dataset of monthly climate and climatic water balance from 1958–2015. *Scientific Data*, 5, 170191.

Assmann, E. (1970). *The principles of forest yield study. Studies in the organic production, structure, increment and yield of forest stands.*

Berdanier, A.B. & Clark, J.S. (2016). Divergent reproductive allocation trade-offs with canopy exposure across tree species in temperate forests. *Ecosphere*, 7, e01313–n/a.

Bogdziewicz, M., Fernández-Martínez, M., Espelta, J.M., Ogaya, R. & Penuelas, J. (2020a). Is forest fecundity resistant to drought? Results from an 18-yr rainfall-reduction experiment. *New Phytologist*, 227, 1073–1080.

Bogdziewicz, M., Kelly, D., Thomas, P.A., Lageard, J.G. & Hacket-Pain, A. (2020b). Climate warming disrupts mast seeding and its fitness benefits in European beech. *Nature Plants*, 6, 88–94.

Brienen, R.J., Caldwell, L., Duchesne, L., Voelker, S., Barichivich, J., Baliva, M. *et al.* (2020). Forest carbon sink neutralized by pervasive growth-lifespan trade-offs. *Nature Communications*, 11, 1–10.

Caignard, T., Kremer, A., Firmat, C., Nicolas, M., Venner, S. & Delzon, S. (2017). Increasing Spring Temperatures Favor Oak Seed Production in Temperate Areas. *Scientific Reports*, 7, 1–8.

Chu, C., Lutz, J.A., Král, K., Vrška, T., Yin, X., Myers, J.A. *et al.* (2019). Direct and indirect effects of climate on richness drive the latitudinal diversity gradient in forest trees. *Ecology Letters*, 22, 245–255.

Clark, J.S. (1990a). Integration of ecological levels: Individual plant growth, population mortality and ecosystem processes. *Journal of Ecology*, 78, 275–299.

Clark, J.S. (1990b). Landscape interactions among nitrogen mineralization, species composition, and long-term fire frequency. *Biogeochemistry*, 11, 1–22.

Clark, J.S., Andrus, R., Aubry-Kientz, M., Bergeron, Y., Bogdziewicz, M., Bragg, D.C. *et al.* (2021). Continent-wide tree fecundity driven by indirect climate effects. *Nature Communications*, 12, 1–11.

Clark, J.S., Bell, D.M., Kwit, M.C. & Zhu, K. (2014). Competition-interaction landscapes for the joint response of forests to climate change. *Global Change Biology*, 20, 1979–1991.

Clark, J.S., LaDeau, S. & Ibanez, I. (2004). Fecundity of trees and the colonization-competition hypothesis. *Ecological Monographs*, 74, 415–442.

Clark, J.S., Nuñez, C.L. & Tomasek, B. (2019). Foodwebs based on unreliable foundations: spatiotemporal masting merged with consumer movement, storage, and diet. *Ecological Monographs*, 89, 1–24.

Corlett, R.T. (2013). The shifted baseline: Prehistoric defaunation in the tropics and its consequences for biodiversity conservation. *Biological Conservation*, 163, 13–21.

Dawkins, R. & Krebs, J.R. (1979). Arms races between and within species. *Proceedings of the Royal Society of London. Series B, Biological Sciences*, 205, 489–511.

Del Grosso, S., Parton, W., Stohlgren, T., Zheng, D., Bachelet, D., Prince, S. *et al.* (2008). Global Potential Net Primary Production Predicted from Vegetation Class, Precipitation, and Temperature. *Ecology*, 89, 2117–2126.

Farr, T.G., Rosen, P.A., Caro, E., Crippen, R., Duren, R., Hensley, S. *et al.* (2007). The shuttle radar topography mission. *Reviews of Geophysics*, 45.

Fisher, R.A., Koven, C.D., Anderegg, W.R., Christoffersen, B.O., Dietze, M.C., Farrior, C.E. *et al.* (2018). Vegetation demographics in Earth System Models: A review of progress and priorities. *Global Change Biology*, 24, 35–54.

Fridley, J.D. (2017). Plant energetics and the synthesis of population and ecosystem ecology. *Journal of Ecology*, 105, 95–110.

Gesch, D., Oimoen, M., Greenlee, S., Nelson, C., Steuck, M. & Tyler, D. (2002). The National Elevation Dataset. In: *Photogrammetric Engineering and Remote Sensing*. American Society for Photogrammetry and Remote Sensing, vol. 68, pp. 5–11.

Green, P.T., Harms, K.E. & Connell, J.H. (2014). Nonrandom, diversifying processes are disproportionately strong in the smallest size classes of a tropical forest. *Proceedings of the National Academy of Sciences*, 111, 18649–18654.

Gruntman, M., Groß, D., Májeková, M. & Tielbörger, K. (2017). Decision-making in plants under competition. *Nature Communications*, 8, 2235.

Hanbury-Brown, A., Ward, R. & Kueppers, L.M. (2022). Future forests within earth system models: regeneration processes critical to prediction. *New Phytologist*, in press, 000–000.

Hargreaves, A.L., Suárez, E., Mehltreter, K., Myers-Smith, I., Vanderplank, S.E., Slinn, H.L. *et al.* (2019). Seed predation increases from the Arctic to the Equator and from high to low elevations. *Science Advances*, 5, 1–11.

Harms, K.E., Wright, S.J., Calderón, O., Hernández, A. & Herre, E.A. (2000). Pervasive density-dependent recruitment enhances seedling diversity in a tropical forest. *Nature*, 404, 493–495.

Hazelton, P. & Murphy, B. (2007). *Interpreting soil test results: What do all the numbers mean?* CSIRO publishing.

Hengl, T., De Jesus, J.M., Heuvelink, G.B., Gonzalez, M.R., Kilibarda, M., Blagotić, A. *et al.* (2017). SoilGrids250m: Global gridded soil information based on machine learning. *PLoS ONE*, 12.

Hille Ris Lambers, J., Clark, J.S. & Beckage, B. (2002). Density-dependent mortality and the latitudinal gradient in species diversity. *Nature*, 417, 732–735.

Janzen, D. (1970). Herbivores and the number of tree species in tropical forests. *The American Naturalist*, 104, 501–528.

Karger, D.N., Conrad, O., Böhner, J., Kawohl, T., Kreft, H., Soria-Auza, R.W. *et al.* (2017). Climatologies at high resolution for the earth's land surface areas. *Scientific Data*, 4, 1–20.

Kattge, J., Bönisch, G., Díaz, S., Lavorel, S., Prentice, I.C., Leadley, P. *et al.* (2020). TRY plant trait database – enhanced coverage and open access. *Global Change Biology*, 26, 119–188.

King, D.A., Davies, S.J., Tan, S. & Md. Noor, N.S. (2009). Trees approach gravitational limits to height in tall lowland forests of malaysia. *Functional Ecology*, 23, 284–291.

Koch, G.W., Sillett, S.C., Jennings, G.M. & Davis, S.D. (2004). The limits to tree height. *Nature*, 428, 851–854.

Koenig, W.D. (2021). A brief history of masting research. *Philosophical Transactions of the Royal Society B: Biological Sciences*, 376, 20200423.

Krinner, G., Viovy, N., de Noblet-Ducoudré, N., Ogée, J., Polcher, J., Friedlingstein, P. *et al.* (2005). A dynamic global vegetation model for studies of the coupled atmosphere-biosphere system. *Global Biogeochemical Cycles*, 19, 1–33.

LaMontagne, J.M., Pearse, I.S., Greene, D.F. & Koenig, W.D. (2020). Mast seeding patterns are asynchronous at a continental scale. *Nature Plants*, 6, 460–465.

Lauder, J.D., Moran, E.V. & Hart, S.C. (2019). Fight or flight? potential tradeoffs between drought defense and reproduction in conifers. *Tree Physiology*, 39, 1071–1085.

Levi, T., Barfield, M., Barrantes, S., Sullivan, C., Holt, R.D. & Terborgh, J. (2019). Tropical forests can maintain hyperdiversity because of enemies. *Proceedings of the National Academy of Sciences*, 116, 581–586.

Lewis, S.L., Phillips, O.L., Sheil, D., Vinceti, B., Baker, T.R., Brown, S. *et al.* (2004). Tropical forest tree mortality, recruitment and turnover rates: Calculation, interpretation and comparison when census intervals vary. *Journal of Ecology*, 92, 929–944.

Locosselli, G.M., Brienen, R.J.W., Leite, M.d.S., Gloor, M., Krottenthaler, S., Oliveira, A.A.d. *et al.* (2020). Global tree-ring analysis reveals rapid decrease in tropical tree longevity with temperature. *Proceedings of the National Academy of Sciences*, 117, 33358–33364.

Mendoza, I., Condit, R.S., Wright, S.J., Caubère, A., Châtelet, P., Hardy, I. *et al.* (2018). Inter-annual variability of fruit timing and quantity at Nouragues (French Guiana): insights from hierarchical Bayesian analyses. *Biotropica*, 50, 431–441.

Minor, D.M. & Kobe, R.K. (2019). Fruit production is influenced by tree size and size-asymmetric crowding in a wet tropical forest. *Ecology and Evolution*, 9, 1458–1472.

Mokany, K., Prasad, S. & Westcott, D.A. (2014). Loss of frugivore seed dispersal services under climate change. *Nature Communications*, 5, 3971.

Moles, A.T., Wright, I.J., Pitman, A.J., Murray, B.R. & Westoby, M. (2009). Is there a latitudinal gradient in seed production? *Ecography*, 32, 78–82.

Obeso, J.R. (2002). The costs of reproduction in plants. *New Phytologist*, 155, 321–348.

Olson, D.M., Dinerstein, E., Wikramanayake, E.D., Burgess, N.D., Powell, G.V., Underwood, E.C. *et al.* (2001). Terrestrial ecoregions of the world: A new map of life on Earth. *BioScience*, 51, 933–938.

Ostfeld, R.S. & Keesing, F. (2000). Pulsed resources and community dynamics of consumers in terrestrial ecosystems. *Trends in Ecology and Evolution*, 15, 232–237.

Pearse, I.S., LaMontagne, J.M., Lordon, M., Hipp, A.L. & Koenig, W.D. (2020). Biogeography and phylogeny of masting: do global patterns fit functional hypotheses? *New Phytologist*, 227, 1557–1567.

Phillips, O.L. & Gentry, A.H. (1994). Increasing turnover through time in tropical forests. *Science*, 263, 954–958.

Pincheira-Donoso, D. & Hunt, J. (2015). Fecundity selection theory: Concepts and evidence. *Biological reviews of the Cambridge Philosophical Society*, 92.

Qiu, T., Aravena, M.C., Andrus, R., Ascoli, D., Bergeron, Y., Berretti, R. *et al.* (2021). Is there tree senescence? The fecundity evidence. *Proceedings of the National Academy of Sciences of the United States of America*, 118, 1–10.

R Core Team (2020). *R: A Language and Environment for Statistical Computing*. R Foundation for Statistical Computing, Vienna, Austria.

Rosenblatt, A.E. & Schmitz, O.J. (2016). Climate change, nutrition, and bottom-up and top-down food web processes. *Trends in Ecology and Evolution*, 31, 965–975.

Running, S.W., Nemani, R.R., Heinsch, F.A., Zhao, M., Reeves, M. & Hashimoto, H. (2004). A continuous satellite-derived measure of global terrestrial primary production. *BioScience*, 54, 547–560.

Sala, A., Hopping, K., McIntire, E.J.B., Delzon, S. & Crone, E.E. (2012). Masting in whitebark pine (pinus albicaulis) depletes stored nutrients. *New Phytologist*, 196, 189–199.

Schemske, D.W., Mittelbach, G.G., Cornell, H.V., Sobel, J.M. & Roy, K. (2009). Is there a latitudinal gradient in the importance of biotic interactions? *Annual Review of Ecology, Evolution, and Systematics*, 40, 245–269.

Sharma, S., Bergeron, Y., Bogdziewicz, M., Bragg, D., Brockway, D., Cleavitt, N. *et al.* (2021). North american tree migration paced by recruitment through contrasting east-west mechanisms. *Proceedings of the National Academy of Sciences*, in press.

Sitch, S., Friedlingstein, P., Gruber, N., Jones, S.D., Murray-Tortarolo, G., Ahlström, A. *et al.* (2015). Recent trends and drivers of regional sources and sinks of carbon dioxide. *Biogeosciences*, 12, 653–679.

Sitch, S., Smith, B., Prentice, I.C., Arneth, A., Bondeau, A., Cramer, W. *et al.* (2003). Evaluation of ecosystem dynamics, plant geography and terrestrial carbon cycling in the LPJ dynamic global vegetation model. *Global Change Biology*, 9, 161–185.

Stephenson, N.L. & Van Mantgem, P.J. (2005). Forest turnover rates follow global and regional patterns of productivity. *Ecology Letters*, 8, 524–531.

Terborgh, J. (1986). *Community aspects of frugivory in tropical forests*, Springer, Dordrecht, vol. 15 of *Tasks for Vegetation Science*.

Tobin, B.Y.J. (1985). Estimation of Relationships for Limited Dependent Variables. *Econometrica*, 26, 24–36.

Vacchiano, G., Ascoli, D., Berzaghi, F., Lucas-Borja, M.E., Caignard, T., Collalti, A. *et al.* (2018). Reproducing reproduction: How to simulate mast seeding in forest models. *Ecological Modelling*, 376, 40–53.

Westoby, M., Jurado, E. & Leishman, M. (1992). Comparative evolutionary ecology of seed size. *Trends in Ecology and Evolution*, 7, 368–372.

Whitham, T.G., Allan, G.J., Cooper, H.F. & Shuster, S.M. (2020). Intraspecific genetic variation and species interactions contribute to community evolution. *Annual Review of Ecology, Evolution, and Systematics*, 51, 587–612.

Yeoh, S.H., Satake, A., Numata, S., Ichie, T., Lee, S.L., Basherudin, N. *et al.* (2017). Unravelling proximate cues of mass flowering in the tropical forests of South-East Asia from gene expression analyses. *Molecular Ecology*, 26, 5074–5085.

Acknowledgements

Competing interests

The authors declare no competing interests
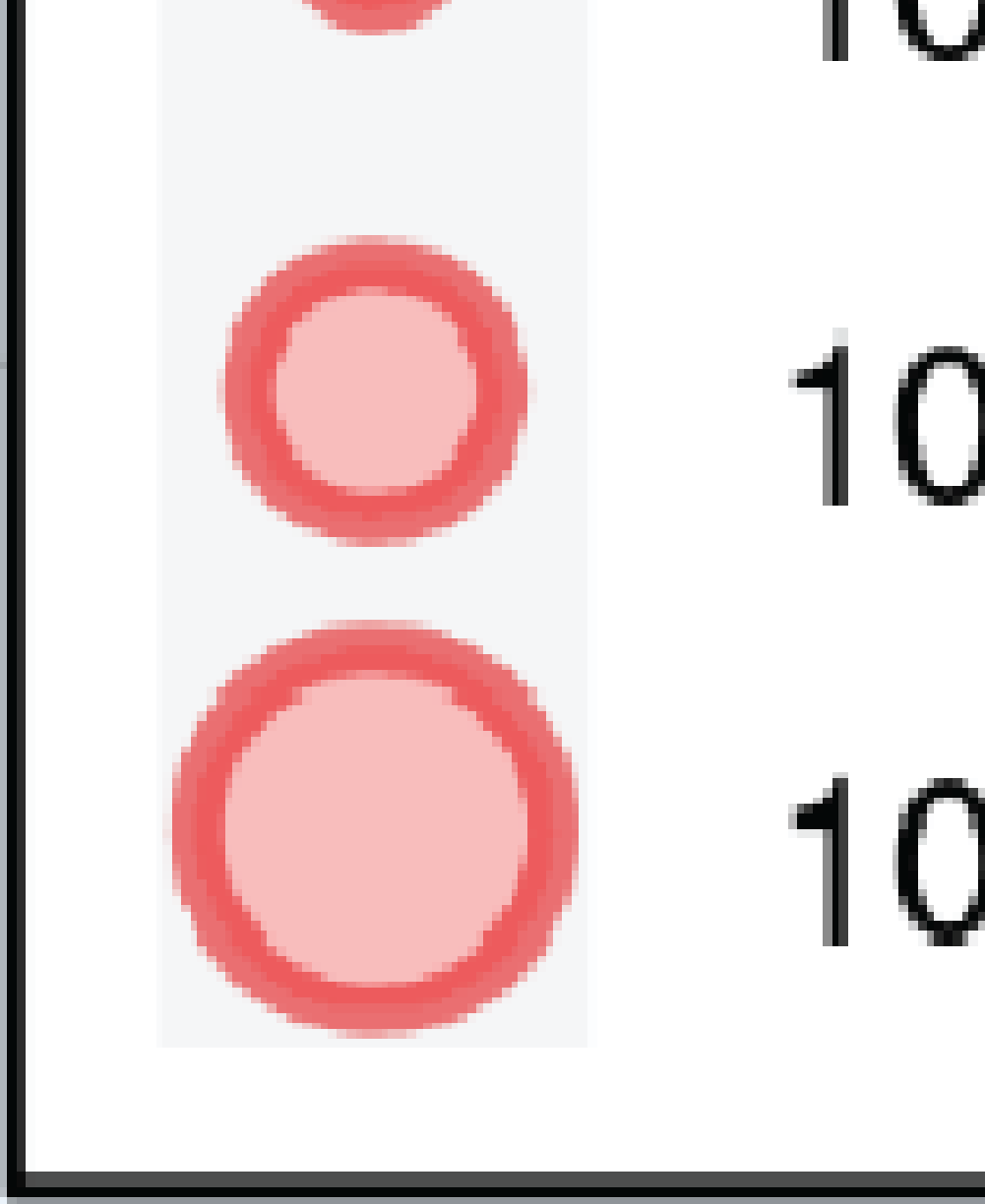
Supporting Information

Table S1 – S3

Fig S1 - S7

Figure 1: a) Individual seed productivity (ISP, seed mass per tree basal area) might not vary with latitudinal climate gradients, in which case community seed productivity (CSP, seed mass production per forest area) depends on variation in tree size. Alternatively, responses could depend on net primary productivity (NPP), increasing if allocation in warm climates shifts preferentially to fecundity or decreasing if allocation in warm climates shifts to growth and defenses. b) Proportionate differences in fecundity hypothesized for the three scenarios in (a) shown as differences from the climate gradient in NPP. The NPP-scaling scenario means that NPP and CSP follow the same proportionate trajectory (green line).
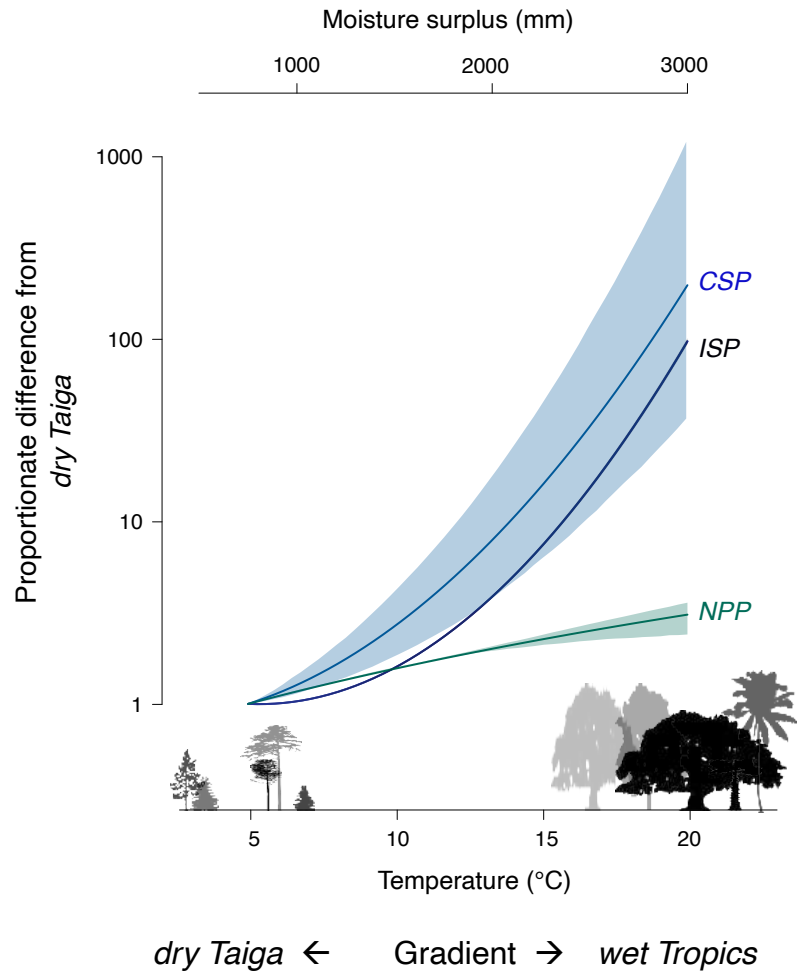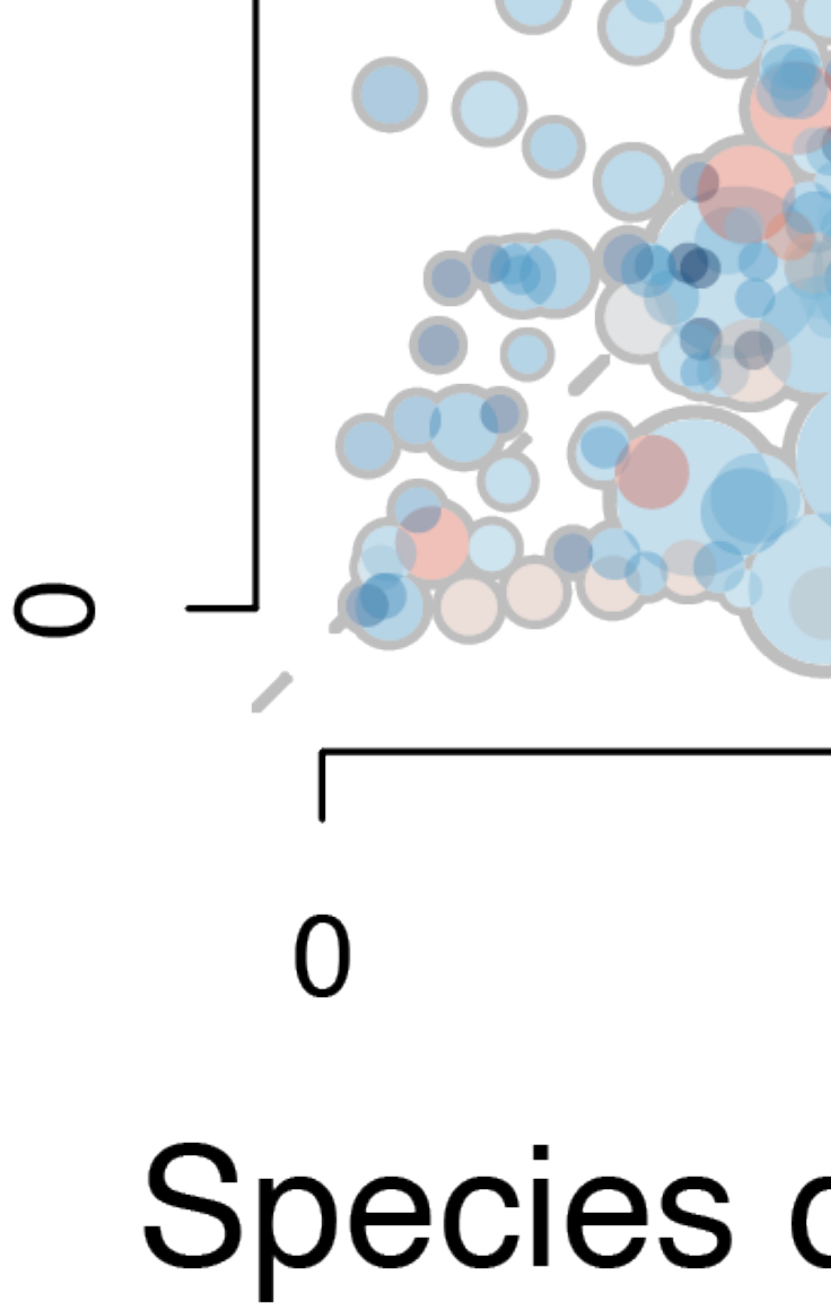
Figure 2: MASTIF data summary, with symbol size proportional to observations. The distribution of data is detailed in Figure S1 and in Table S1.

Figure 3: The MASTIF model simplified from Clark *et al.* (2019) to emphasize variables and parameters discussed in the text. A biophysical model for change in fecundity $\psi_{i,t}$ of tree i in year t (a tree-year) is driven by individual tree condition and climate and habitat variables in design vector $\mathbf{x}_{i,t}$ with corresponding coefficients $\boldsymbol{\beta}$. Maturation status incorporates tree diameter $d_{i,t}$. The hierarchical state-space model includes process error variance σ^2 and observation error in two data types. A crop count $c_{i,t}$ has a beta-binomial distribution that includes observation error through the estimated crop fraction. A set of seed traps provides a vector of counts $\mathbf{y}_t = y_{1,t}, \dots, y_{n,t}$ that together provide information on tree i through a dispersal kernel. There is conditional independence in fecundity values between trees and within trees over time, taken up by stochastic treatment of $\psi_{i,t}$. There is an additional subscript for location j that is suppressed here to reduce clutter. The full model includes additional elements (see Model Inference with MASTIF).

Figure 4: a) Climate responses for (a) ISP (seed production per tree basal area, log10 g m^{-2} y^{-1}) (b) CSP (seed mass per ha forest floor, log10 g ha^{-1} y^{-1}), and (c) NPP (kg C m^{-2} y^{-1}). Dashed lines indicate the transect from dry taiga to wet tropics in Fig. 5b. The scales for contours are linear for (c) and log$_{10}$ for (a) and (b). Convex hulls are defined by observations (red), including individual trees (a, c) and inventory plots (b). Surface predictive standard error are reported in Figure S3. Coefficients are reported in Table S3.

Figure 5: a) Two order of magnitude increases from cold/dry to warm/moist for individual (ISP) and community (CSP) seed production relative to NPP. Curves are sections through surfaces (dashed lines) in Fig. 4, with scales for moisture surplus (above) and temperature (below). Curves are in proportion to values in cold, dry conditions. Confidence intervals (95%) are not visible for ISP and NPP due to the large number of trees. Confidence intervals are wider for CSP due to limited inventory plots at high temperatures (Fig. 2).

Figure 6: Species diversity in seeds (vertical axis) is lower than expected from species diversity in trees (horizontal axis). In both cases, diversity is evaluated from the Shannon index, $-\sum_s p_s \log p_s$, where p_s is the fraction of species s in basal area (trees) and CSP (seed mass). Each point represents an inventory plot. Except at low tree diversity, points lie almost entirely below the 1:1 line (dashed). The legend at top left shows mean annual temperature (symbol color) and mass of the average seed (symbol size).

Supporting Information

Globally, tree fecundity exceeds productivity gradients

Valentin Journé *et al.*, Ecology Letters

This Supplement provides additional data summaries as tables and figures. Full summaries of the MASTIF network are available these links for sites and species.

Supplementary Tables

Table S1: Numbers of species, stands, trees, and tree-years for ISP analysis and complete inventories for CSP analysis by tropical and temperate regions. Complete inventories include all trees within a mapped plot and are needed to determine seeds per area in CSP. Because not all inventory plots use the same minimum diameter, the latter is based on trees > 7 cm.

Floristic Region	Species	Sites	Tree-years	Trees	Complete inventories
Tropical	559	64	9,723,438	85,261	47
Temperate	194	3506	2,330,294	61,461	204

Table S2: Covariates used to fit the MASTIF model and data sources. Subscripts are tree i, site j, and year t.

Covariate	Units	Data source
Diameter ($G_{ij,t}$, $G_{ij,t}^2$)	cm, cm^2	MASTIF
Crown class ($C_{ij,t}$)	ordinal (class 1-5)	MASTIF
Moisture surplus (S_j)	mm	terraClimate, CHELSA
Surplus anomaly ($S_{j,t}$)	mm	terraClimate, CHELSA
Temperature (T_j)	°C	terraClimate, CHELSA
Temperature anomaly ($T_{j,t}$)	°C	terraClimate, CHELSA
$S_j \times G_{ij,t}$	mm × cm	
CEC$_j$ (0 - 30cm)	mmolc/kg	soilgrid250m
Slope, aspect (u_{1j}, u_{2j}, u_{3j})	radians	DEM, USGS

Table S3: Coefficients for climate effect on individual (ISP), community fecundity (CSP) and on NPP (MODIS or DGVMs TRENDY). ISP and CSP fecundity are fitted on a natural log scale. r^2 for ISP = 0.2, CSP = 0.15, NPP MODIS = 0.48, NPP DGVM = 0.52.
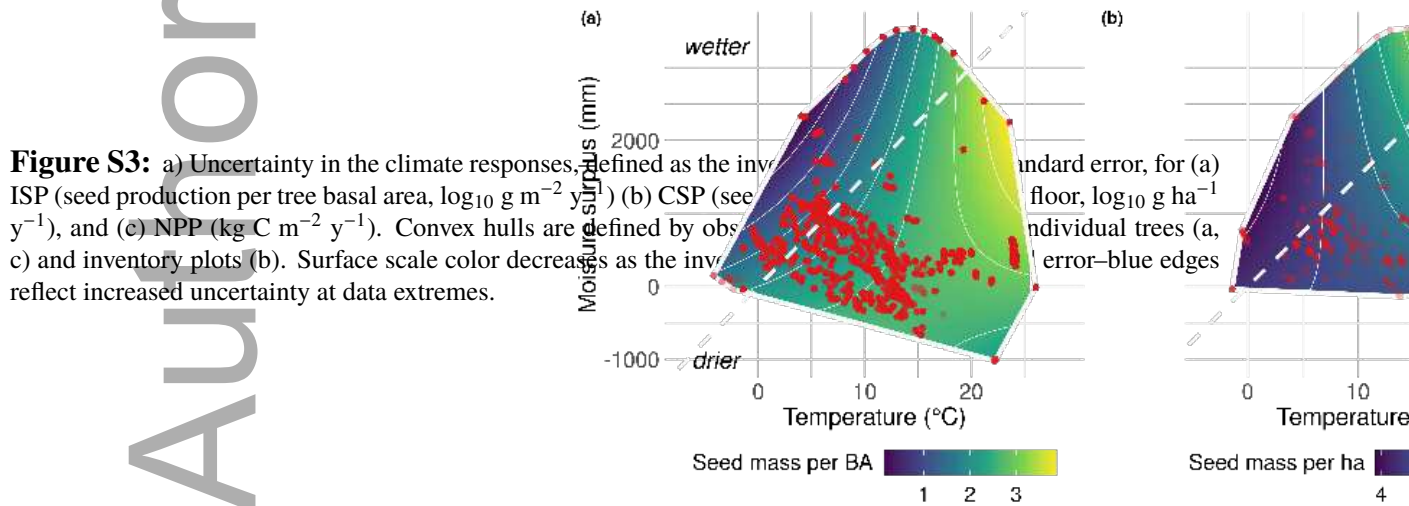
Variable	Estimate	SE	P-value
Climate effects on $\log_e$ISP			
Intercept	4.64e+00	4.93e-02	<2e-16
T	1.78e-01	6.01e-03	<2e-16
T^2	-5.60e-03	1.770e-04	<2e-16
S	-2.72e-03	4.80e-05	<2e-16
S^2	-1.12e-07	1.14e-08	<2e-16
$T \times S$	1.84e-04	1.73e-06	<2e-16
Climate effects on $\log_e$CSP			
Intercept	9.88e+00	5.61e-01	<2e-16
T	9.96e-02	7.88e-02	0.21
T^2	-2.38e-03	2.82e-03	0.40
S	-9.21e-04	7.16e-04	0.20
S^2	2.87e-08	2.20e-07	0.90
$T \times S$	1.19e-04	4.05e-05	3.60e-3
Climate effects on NPP (MODIS)			
Intercept	3.52e-01	2.46e-02	< 2e-16
T	1.54e-02	1.92e-03	5.18e-15
S	1.80e-04	3.34e-05	1.02e-07
$T \times S$	1.12e-05	2.64e-06	2.41e-05
Climate effects on NPP (DGVMs TRENDY)			
Intercept	1.455e-01	2.2e-02	7.71e-11
T	3.19e-02	1.72e-03	< 2e-16
S	3.25e-04	3.00e-05	< 2e-16
$T \times S$	-7.36e-06	2.38e-06	0.00199

Supplementary Figures

Figure S1: MASTIF data network, including longitudinal (green) and opportunistic (orange) observations in North America (a), Europe (b), Asia (c), South and Central America (d), Africa (e) and Oceania (f). Dot size represents the number of initial tree year observations at log10 scale. Numbers of observations are reported in Table S1.

Figure S2: Climate responses for ISP (seed mass per basal area) (a, b, c) and stand-level CSP, as g ha^{-1} (d, e, f) showing marginal responses to temperature (a and d) and moisture surplus (d and e) with observations (dots) and the fitted model, and interactions between temperature and moisture surplus (c and f). Coefficient are reported in Table S3. Low and high values used for conditional plots in (c and f), labelled as Moist ($S = 1500$ mm) and Dry ($S = -50$ mm). Due to large sample size, confidence intervals around lines in (a, b, c) are not distinct from the predictive mean. Temperature and moisture surplus correspond here to a mean annual value for each sites.

Figure S3: a) Uncertainty in the climate responses, defined as the inv[...] [...]ndard error, for (a) ISP (seed production per tree basal area, $\log_{10}$ g m^{-2} y^{-1}) (b) CSP (see [...] floor, $\log_{10}$ g ha^{-1} y^{-1}), and (c) NPP (kg C m^{-2} y^{-1}). Convex hulls are defined by obs[...] [...]ndividual trees (a, c) and inventory plots (b). Surface scale color decreases as the inv[...] [...] error–blue edges reflect increased uncertainty at data extremes.

Figure S4: Because BCI includes the largest sample of tree years, we show that the same trend exists without BCI for both (a) ISP, (seed production per tree basal area, $\log_{10}$ values) and (b) CSP (seed mass per ha forest floor, $\log_{10}$ values).
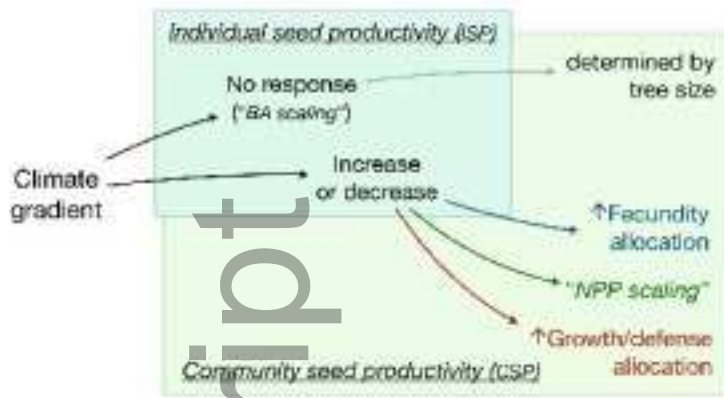
Figure S6: Relationships between NPP from MODIS and individual (standardized) fecundity ISP (a) and stand CSP (b), both positive ($p < 0.00001$) and both accounting for little of the variability ($r^2 = 0.05$ and 0.13, respectively).
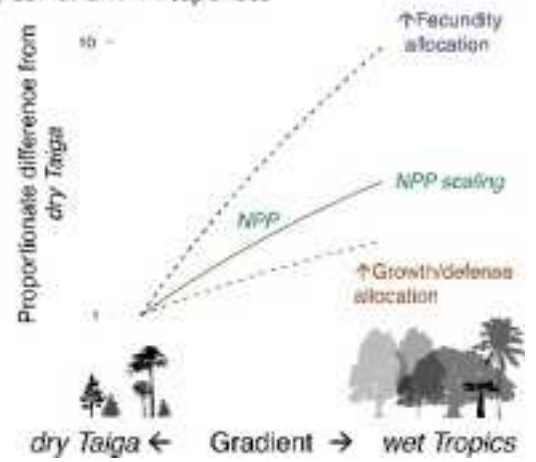
0
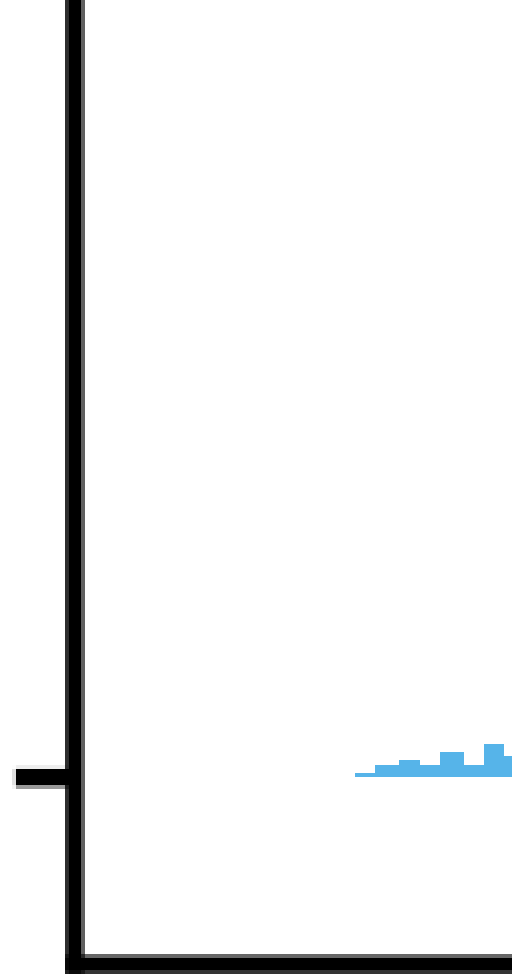
Figure S7: Distribution of (a) ISP (g seed per m^2 basal area) and (b) CSP (g seed per ha basal area) fecundities. Black dotted lines represent the quantile at 2.5 and 97.5%.

a) Individual and community response

Individual seed productivity (ISP)

No response ("BA scaling") → determined by tree size

Climate gradient → Increase or decrease → ↑Fecundity allocation → "NPP scaling" → ↑Growth/defense allocation

Community seed productivity (CSP)

b) CSP and NPP responses

Proportionate difference from dry Taiga

↑Fecundity allocation
NPP scaling
NPP
↑Growth/defense allocation

dry Taiga ← Gradient → wet Tropics

ele_14012_f1.png
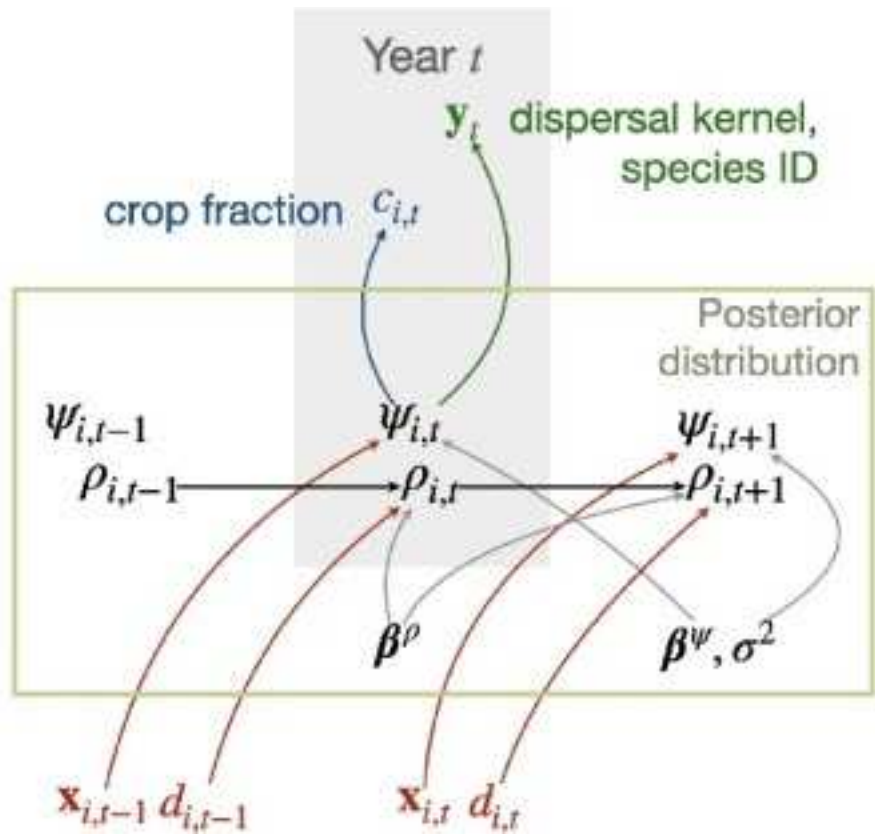
ele_14012_f2.png

ele_14012_f3.png

ele_14012_f4.png

Moisture surplus (mm)

Proportionate difference from *dry Taiga*

Temperature (°C)

dry Taiga ← Gradient → *wet Tropics*

Species diversity in seed mass

Species diversity in tree basal area

°C (color scale)

g/seed (size scale)

22   6
14   2
6   0.1

ele_14012_f6.png